DOI: https://doi.org/10.24297/rv1nsa89

Persistent Homology Of Metric Expanders: Stability, Collapse, And Dimensional Reduction

Marwa Q. Atshan

Department of Mathematics,

University of Al-Qadisiya, College of Education,

marwa.atshan@qu.edu.iq

https://orcid.org/0009-0002-0506-0064

ABSTRACT

Persistent homology provides a multi-scale framework for characterising topological structure. Nonetheless, its behaviour in highly-expanding graph-induced metric spaces is still not well-understood. This study shows that some causal structures exhibit metric expansion as a stability mechanism, which is closely related to the persistent homological structure. A graph-modeling mathematical–computational framework was applied to 152 graph instances, namely 40 controlled expanders, 24 controlled non-expanders, and 88 real-network validation samples. The shortest-path metrics and the normalized Laplacian spectral gaps were assessed. This was followed by Vietoris–Rips persistent homology in H_0 and H_1 for all cases and H_2, whenever computationally feasible. The study focused on persistence diagrams, barcodes, Betti curves, lifetime-based measures, entropy, collapse scales, and operational dimensional measures, as well as bottleneck and Wasserstein distances. Controlled expanders have significantly higher mean H_1total persistence (71.2750) than do non-expanders (20.0417), but earlier mean H_1collapse (2.6750 versus 5.9583). Samples taken from the real networks had a smaller mean H_1total persistence (1.5568) despite having a larger mean spectral gap (0.3206), thus showing that the mean spectral gap cannot be taken as the only reason for any persistent-topological complexity due to the presence of special features in real networks. Over the course of 240 perturbation runs, we see that the mean bottleneck distance increased from 0.015 to 0.147 while the mean Wasserstein distance increased from 0.34 to 3.44 as the perturbation magnitude increased from 0.01 to 0.10. This implies a smooth stability response. The research findings indicate that expansion and persistent topology are systematically related, but not through some universal monotonic relation; they are conditioned by graph family and metric organization. Collapse is also conditioned, as well as effective dimension structure.

Keywords: Persistent Homology; Metric Expanders; Vietoris–Rips Complex; Persistence Diagrams; Topological Data Analysis; Stability; Dimensional Reduction.

1. INTRODUCTION

Persistence homology plays an important role in topological data analysis (TDA) for studying structural properties at various scales. With the use of filtration, connected components, cycles, and high dimensional objects may be studied in terms of their births and deaths by means of persistence diagrams and barcodes. Recent advances in Vietoris–Rips persistence homology have shed some light on its relation to geometry of metric spaces in general (Lim et al., 2024).

Metric spaces induced by graphs offer a convenient framework for such analysis. Any connected graph may be viewed as a metric space based on shortest-path distance, which in turn allows for Vietoris–Rips filtration of the graph's connectivity, cycles, and other topological properties.

1.1 Persistent Homology and Topological Data Analysis

The persistence homology technique builds on traditional homology methods by noting at what scale these topological properties continue to exist. The persistence diagrams, barcodes, Betti curves, and the durations of the features thus indicate both the number of multiscale structures and how long-lived they are.

Regarding graph distances, raising the filtration scale increasingly converts the pairwise distance relations between points into more complex simplicial structures. This implies that Vietoris–Rips complexes are very significant from the perspective of relating metric geometry to graph topology (Oudot & Solomon, 2021).

1.2 Metric Spaces and Expander Graphs

The expander graphs have sparsity of local structure and high level of global connectivity. Expansion in expander graphs can be analyzed from spectral perspective, while the shortest paths distribution and the diameter of expander graphs determine their metric properties. The random regular graphs are especially important since their spectral gap determines measures of expansion (Sarid, 2023).

Spectral expansion is not sufficient to fully capture topological properties of graphs. Graphs can be quite similar in their global metric properties but different in terms of their cycles. Therefore, this paper examines the issue of expansion in relation to graph order, degree, diameter, distance distribution, and persistence properties.

1.3 Expansion and Topological Complexity

Expansivity and persistent topology are not always monotonic together. Strong connectivity could reduce distances within the graph and lead to faster generation of simplices, such that cycles disappear already at smaller filtration values, while on the other hand, sparse expanding graphs can have many cycles at the early stages of the filtration process.

Such a difference in the effect of expansivity from persistence lifetime and collapse scale prompts joint study of persistence abundance, feature lifetime, homological collapse, topological complexity and metric stability.

1.4 Research Gap and Problem Statement

Despite considerable theoretical backing for persistent homology, Vietoris–Rips topology, metric graph theory, and spectral expansion, little is known about the collective behavior of these concepts concerning feature structure persistence, homological collapse, metric stability, and effective dimensionality.

This work will thus examine the influence of graph-induced metric space expansions on the Vietoris–Rips persistent homology structure. In particular, the following topics will be covered: positive dimensional persistent structures, homological collapse between scales of filtration, diagram stability to metric perturbations, and distribution of persistent information over homological dimensions.

1.5 Study Contributions

The contribution of this work is the development of a joint mathematical/computational approach to the comparison of persistent topology for families of expanders and non-expanders, externally validated with real-world networks. This work not only assesses the significance of each of these features but also characterizes topological dimension from the perspective of persistence summaries and dimensionality reduction.

Together, all of these approaches link spectral expansion, metric geometry induced by graphs, and persistent topology.

2. LITERATURE REVIEW

The research related to metric expanders and persistent homology includes topological data analysis, Vietoris–Rips topology, spectral graph theory, metric geometry, persistence stability, and dimension reduction. These disciplines together constitute the theory which underlies the study of how graph connectivity and metric structure affect multiscale topology.

2.1 Persistent Homology

Persistence homology captures topological features at various scales of filtration, where such features are characterized by their births, persistences, and deaths using intervals, persistence diagrams, and persistence barcodes. This technique is especially applicable in the case of finite metric spaces since it does not depend on one fixed threshold value. Advancements in computation algorithms have made Vietoris-Rips persistence more feasible to compute. Ripser by Bauer (2021) is a computationally efficient approach to calculate Vietoris-Rips persistence barcodes.

2.2 Vietoris–Rips and Čech Complexes

Vietoris-Rips and Čech complexes convert metric relations into simplicial complexes. While Čech complexes are defined using intersections of metric balls, Vietoris-Rips complexes rely on distances between points, thus being especially useful for finite graph metrics. The topology that results from this procedure is still strongly related to the geometry. Majhi (2023) studied Vietoris-Rips complexes of metric spaces close to metric graphs, whereas Chachólski et al. (2021) considered homotopy decompositions of simplicial and Vietoris-Rips complexes.

2.3 Expander Graphs

Expanders are defined as sparse graphs with very good global connectivity, usually captured via combinatorial or spectral parameters. The spectral gap is especially informative regarding the graph's connectivity and its resistance against partitioning. Brito et al. (2022) studied the spectral gap in random bipartite biregular graphs, while Dinitz et al. (2020) explored approximate Moore graphs and their properties related to expansion and diameter. Wagner (2022) discussed the mathematical background of expanders in higher dimensions. The previous literature highlights the structural importance of expansion without claiming the sole determination of persistence topology by spectral expansion.

2.4 Metric Geometry of Expanders

Shortest path distances permit a graph to be considered as a finite metric space. The diameter and the distance distribution account for the metric organization of a graph, while cycles and local connectivity play an important role in the formation of

the simplicial complexes formed through the filtration process. Adamaszek and Adams (2022) proved that hypercubes have a non-trivial Vietoris-Rips topology, while Shukla (2023) studied the structure of these graphs at scale three. In addition, Adamaszek et al. (2020) proved that Vietoris-Rips homotopy types depend on how metric spaces are glued together.

2.5 Stability of Persistent Homology

The question of persistence stability is about how much metric perturbation leads to controlled perturbation in the corresponding persistence diagram. The bottleneck distance and Wasserstein distance can be regarded as two ways to measure the displacement of persistence diagram by addressing maximal and total difference, respectively. Skraba and Turner (2020) gave stability conditions based on Wasserstein distance for persistence diagram, offering theoretical evidence for the study of persistence with respect to metric perturbation.

2.6 Dimensional Reduction in Topological Data Analysis

TDA dimensionality reduction aims to maintain or capture meaningful topological properties with lower-dimensional representations. Arya et al. (2021) considered the issue of dimensionality reduction in the context of persistent homology, whereas Vipond (2020) introduced the multiparameter persistence landscape method for describing complex persistence data. In the current research, effective dimensionality is considered operationally, not as an intrinsic property of the graph itself. Effective dimensionality is defined based on lifetime-dependent persistence summaries, entropy-based effective numbers of features, persistence feature distribution over homological dimensions, and lower-dimensional structural-persistence representations.

2.7 Research Gap

Previous literature offers extensive evidence regarding Vietoris-Rips topology, graph distance metrics, expansion, stability, and dimensional representations. However, their interrelationships have been studied independently up to now. The interconnection between expansion and the number of persistent features, life time, topological collapse, stability, and dimensionality is still poorly investigated.

The current work is aimed at filling this research gap by means of controlled studies of expander and non-expander graph families, wherein samples of real-life networks are kept aside for an independent external verification. Such an approach allows for studying the relationship between persistent topology and expansion taking into account graph size, degree, shortest-path structure, cycles, and graph family.

3. RESEARCH OBJECTIVES AND QUESTIONS

The investigation explores the connection between metric expansion and persistent topology with a special focus on persistent structure, homological collapse, metric stability, and effective dimensionality.

3.1 Research Objectives

Objectives of the analysis include:

1. To describe the persistent homological structure of metric expanders over different Vietoris-Rips scales.

2. To analyze the stability and collapse of persistent homology in response to changes in metric and expanding behavior.

3. To estimate dimensionality reduction through topological complexity metrics based on persistence.

4. The study uses H_0, H_1 and, where applicable, H_2, along with persistence timescales, entropy and collapse scales.

3.2 Research Questions

The objectives are addressed through three research questions:

RQ1: How does the metric expansion affect persistent homological structures?

RQ2: In which cases will homological collapse happen, and how stable will be the produced persistence diagrams?

RQ3: To which extent persistent homology will detect dimensional reduction in metric expanders?

These research questions together study the effects of expansion on the multiscale topology, the behavior of persistent structures during the process of filtration and perturbation of metrics, and the distribution of persistent structures in homological dimensions.

4. METHODOLOGY

A mathematical-computational experimental setup was applied to investigate the manifestation of spectral expansion via the topological persistence of graph-induced metric spaces. The setup consisted of controlled expander and non-expander graph families alongside a validation set of real-world networks. Graphs were first converted to shortest-path metric spaces, after which persistent homology calculations, stability analysis, collapse analysis, and dimension-complexity calculation took place. The entire controlled experiment consisted of 40 expanders and 24 non-expanders, whereas 88 real-world network samples were left for external validation.

4.1 Research Design

The experiment used a controlled computational approach where the variables of graph order, degree, and type of structure were manipulated. Empirical networks were also analyzed independently since the degree heterogeneity and other properties of these networks were different from the graphs created under the controlled approach. This was necessary for an analysis of the expansion-persistence phenomenon in a controlled setting and not in an empirical network.



Figure 1. Overall computational framework for persistent-homology analysis of metric expanders

4.2 Construction of Metric Expanders

The controlled set was built using the random regular graph and the Margulis-Gabber-Galil graph construction along with path, cycle, grid, and Watts-Strogatz non-expander baseline sets. Graph sizes used were $n = 32, 48, 64,$ and 96, whereas for the random regular graphs, degrees $d = 3, 4,$, and 6 were used. The generated controlled set included 40 expander and 24 non-expander graphs. External validation was done using 88 connected graphs taken from 11 publicly available network matrix datasets that include Epinions, LiveJournal, Pokec, Slashdot, Bitcoin Alpha, Bitcoin OTC, and signed-network data.

4.3 Metric Construction

For each connected graph $G = (E)$, the shortest-path metric was defined as

$$d_G(v) = \min_{P:u \rightsquigarrow v} \sum_{e \in P} w_e, \qquad (1)$$

where Pdenotes a path connecting vertices $u$and v, and $w_e = 1$for the unweighted graph analysis. The graph diameter was computed as

$$diam(G) = \max_{u,v \in V} d_G(v). \qquad (2)$$

Graph structural features that were investigated included order, size, average degree, degree standard deviation, diameter, average distance, and the normalized Laplacian spectral gap. The normalized Laplacian matrix and its second smallest eigenvalue were defined as

$$L_{norm} = I - D^{-1/2} A D^{-1/2}, \ \lambda_2 = \lambda_2\left(L_{norm}\right), \qquad (3)$$

where $A$and Ddenote the adjacency and degree matrices, respectively. Pairwise distances were additionally normalized by $diam(G)$for cross-graph comparison of metric concentration.

4.4 Persistent Homology

Vietoris–Rips persistent homology was computed directly from the shortest-path distance matrices. For a finite metric space $(d)$and filtration scale r, the Vietoris–Rips complex was defined by

$$VR(r) = \left\{\subseteq X: d\left(x_j\right)\leq r\ \forall\, x_i x_j \in \sigma\right\}. \quad (4)$$

The corresponding k-dimensional Betti number at scale $r$was

$$\beta_k(r) = H_k\ (VR(r)). \quad (5)$$

Persistent homology was evaluated in $H_0$and $H_1$for every successfully processed graph, with H_2additionally computed where computationally feasible, principally for $n\leq 64$. For each finite persistence interval $\left(d_i\right)$, the lifetime was $l_i = d_i - b_i$, and total persistence was calculated as

$$TP_k = \sum_{i=1}^{N_k} (d_i - b_i). \quad (6)$$

Persistence entropy was obtained from the normalized lifetimes,

$$p_i = \frac{l_i}{\sum_j l_j},\ E_k = -\sum_i p_i \ln ln\, p_i\,. \quad (7)$$

The operational collapse scale in homological dimension $k$was defined as the final finite death:

$$r_{collapse}^{(k)} = \max_{i:d_i<\infty} d_i. \quad (8)$$

The resulting figures were the number of features, total and average persistence, maximal lifespan, persistence entropy, normalized entropy, and collapse size.

4.5 Stability and Collapse Analysis

The stability of metrics was assessed by introducing perturbations to the length of positive edges. For each value of perturbation ε, the weighted shortest path distance and the respective persistence diagram were recalculated. The obtained H1-diagram was then compared with the diagram for the unperturbed graph using bottleneck and Wasserstein distances. The full experiment included 240 perturbation iterations of 24 sample graphs. Homological collapse was assessed based on the finite death scale (Eq. (8).

4.6 Dimensional Reduction Analysis

Topological complexity was successfully defined in terms of Betti curves, persistence lifetimes, persistence entropy, effective feature number, effective persistent dimension, and a weighted index combining persistence lifetimes and dimensions. Also, principal components of standardized structural and persistence measures were computed in order to obtain an efficient low-dimensional description of the hybrid metric-topological structure. The above features were regarded as operational definitions of the homological information generated.

4.7 Computational Framework

The computational procedure was programmed in Python. Graphs were created and processed using NetworkX, numerical/ spectral analysis was conducted using NumPy and SciPy, while Ripser software and GUDHI compatible procedures were applied for the persistent homology computation/persistence diagram comparison. The statistical testing involved Spearman's rank correlation tests for monotonic relationships, Mann–Whitney U-tests for control expander/non-expander comparison, and HC3 robust ordinary least squares regression models for multivariable sensitivity analysis.

5. DATA COLLECTION AND ANALYSIS

The study combined a controlled graph experiment with independent testing on real networks. Graphs were converted into metric spaces based on the shortest path distances between their vertices and studied via Vietoris–Rips filtrations. A total of 152 successful conversions resulted in the final data set for comparison of spectral expansion, persistence, collapse properties, stability, and effective dimension.

5.1 Graph Generation and External Validation

The controlled experiment involved 64 graphs, 40 expanders and 24 non-expanders, whereas the validation set consisted of 88 examples of real networks derived from Kaggle/SNAP. The average graph order was about 60 nodes for each of the three sets. Table 1 shows the sample properties and spectrum.

Table 1. Experimental sample structure

Experimental role	Graph class	N	Mean n	Mean spectral gap	Median spectral gap
Controlled	Expander	40	59.75	0.2183	0.1876
Controlled	Non-expander	24	60.00	0.0271	0.0213
External validation	Real network	88	60.00	0.3206	0.3507

The control group was highly comparable in terms of graph order but significantly different in spectral gap with values 0.2183 for expanders and 0.0271 for non-expanders. Real networks displayed the largest value of spectral gap (0.3206), implying a unique validation approach.

5.2 Filtration Construction

Each of the graphs was turned into a finite metric space by using the exact all-pairs shortest path distances between them. Vietoris–Rips complexes were tested on the scales produced from the filtration process. The discrete nature of the shortest path metrics resulted in prominent births and deaths happening at integer values.

5.3 Persistent Homology Analysis

Persistence diagrams and barcodes were generated for representative controlled graphs selected near their class medians in spectral gap and H_1 persistence, subject to the presence of H_1 features.

The representative expander, RR_n64_d4_r1, contained 59 H_1 features, H_1 total persistence of 62, maximum H_1 lifetime of 2, and collapse scale of 3. The representative non-expander, WS_n64_r1, contained 12 H_1 features, total persistence of 22, maximum lifetime of 4, and collapse scale of 5. Thus, the size-matched cases differed substantially in feature abundance, longevity, and collapse behaviour.

5.4 Stability Analysis

The metric perturbations were controlled at higher levels of perturbation magnitude. The maximum distortion of the metric along with their corresponding persistence diagram distances were measured. The responses of both bottleneck stability and Wasserstein stability for increasing perturbation were determined. A comparison was made between the bottleneck distance and metric distortion.

5.5 Comparative Analysis

Comparative analysis compared spectral expansion to H_1 persistence and collapse scale, graph size to H_1 persistence, and expansion to persistent dimension. Observations of real networks served as an external reference point but remained separate from the primary comparative analysis. The table below provides summary statistics for the key metrics.

Table 2. Main structural and persistent summaries by graph class

Class	N	Mean degree	Mean λ_2	Mean diameter	Mean H_1 features	Mean H_1 TP	Mean H_1 max life	Mean H_1 collapse
Expander	40	4.5363	0.2183	5.2750	63.0000	71.2750	1.6750	2.6750
Non-expander	24	3.2331	0.0271	22.0417	13.1667	20.0417	5.1250	5.9583
Real network	88	3.6559	0.3206	3.4886	1.5568	1.5568	0.1591	0.3182

Expander graphs showed significantly more H_1 features as well as larger H_1 persistence but had shorter maximum lifetimes compared to the non-expanders, which showed lesser number of H_1 features but with longer lifetimes. Real-world networks fell into another class that had a combination of large spectral gap and small diameter but small H_1 persistence

6. RESULTS

The results reveal significant variations amongst the three sets of networks with regard to their spectral properties, persistence, collapse characteristics, stability, and complexity. The relationship between expansion and persistence was also found to be different in the two studies, implying that spectral expansion is not sufficient for persistent topology.

6.1 Structural Properties of Expanders

The controlled expanders and non-expanders were similar to each other in terms of mean graph order but very different in terms of spectral and metric properties. Mean $\lambda_2$was 0.2183 for controlled expanders but 0.0271 for non-expanders. Their mean diameter was 5.275, while the mean diameter of non-expanders was 22.042. Thus, the controlled comparison highlighted the desired difference in terms of global connectivity and metric geometry. In turn, real networks showed the highest mean spectral gap value, which was 0.3206, along with a low mean diameter, which was 3.489. Yet their heterogeneity and sampling prevented them from falling into the topological category of controlled expanders. The structural characteristics of representative graphs from the three categories are presented in Figure 2.

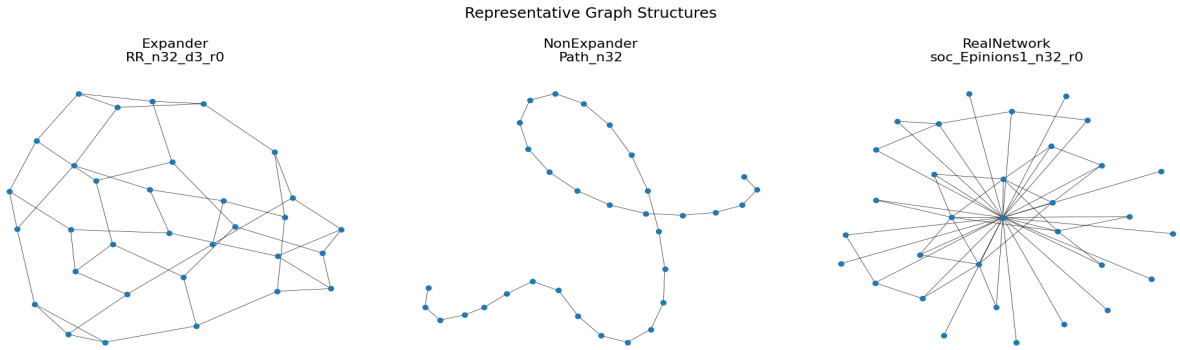

Figure 2. Representative graph structures: controlled expander, controlled non-expander, and real-network validation sample.

Figure 2 shows the difference in the manner in which the graphs are organized. The random-regular expander is sparse but globally well-connected, the non-expander baseline is long metrically organized, and the Epinions-derived real-world network sample has hub-like local organization.

The normalized shortest path distances are shown in Figure 3.

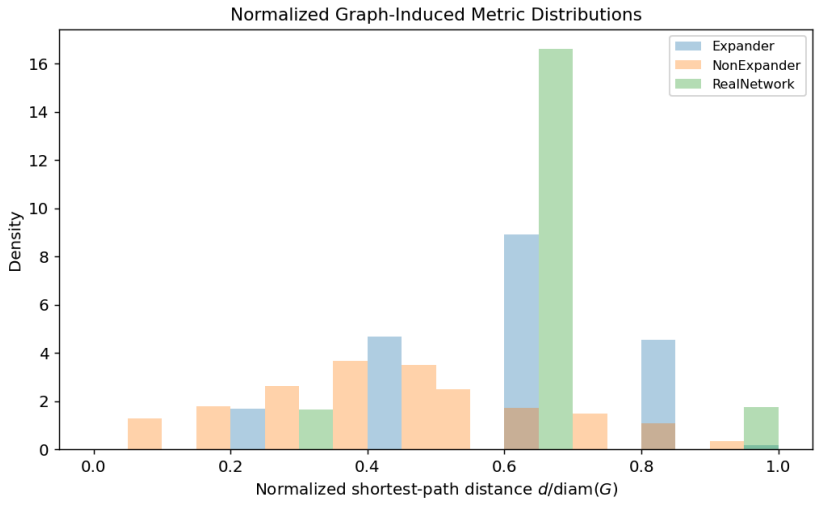

Figure 3. Normalized shortest-path distance distributions for representative graph classes.

The normalizing factor by diameter brings the shortest path distribution to a standard scale of 0 to 1, which makes the comparison of the distribution easier.

The spectral properties of the complete graphs' classes are demonstrated in Fig. 4.

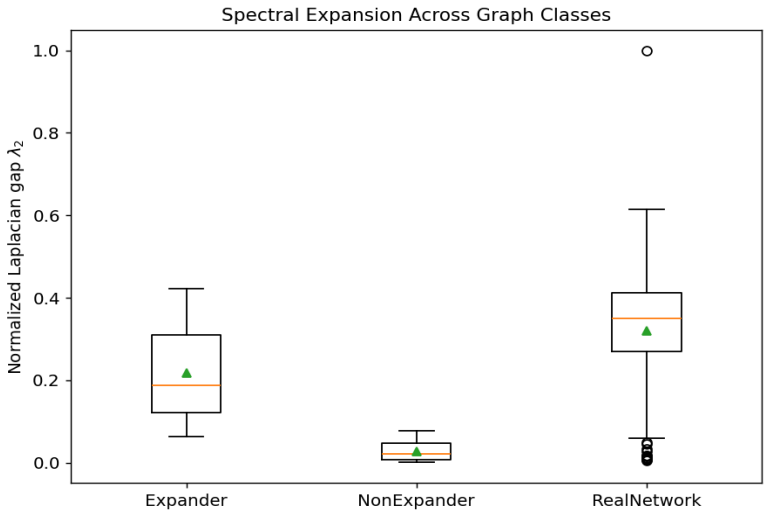

Figure 4. Spectral expansion across graph classes measured by normalized Laplacian λ_2.

Figure 4 illustrates the low spectral expansion of the controlled non-expanders as well as the higher spectral expansion of the controlled expanders. The real network validation sets exhibit significant spectral variability, which further justifies their categorization as a separate external validation component.

6.2 Persistence Diagrams and Barcodes

The representative persistence diagrams show different regimes of multi-scale topologies. The controlled expander consists of a large number of H_1 structures that have emerged at the first non-trivial distance scale, as well as H_2 structures that emerge at the higher distance scale. The representative non-expander contains relatively less H_1 structures, but it does consist of some loops.

These persistent structures are depicted in Figure 5.

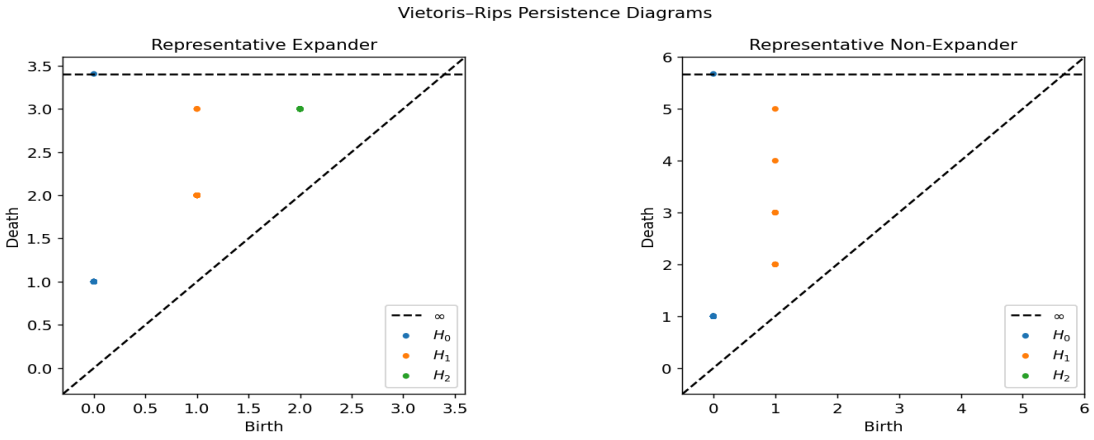

Figure 5. Vietoris–Rips persistence diagrams for the representative controlled expander and non-expander.

The H_1 complexity shown in the persistence diagram is greater for the expander graph as compared to the non-expander, which has lesser number of cycles but with higher lifetime.

Persistence bars in figure 6 below show more analysis of the persistence intervals.

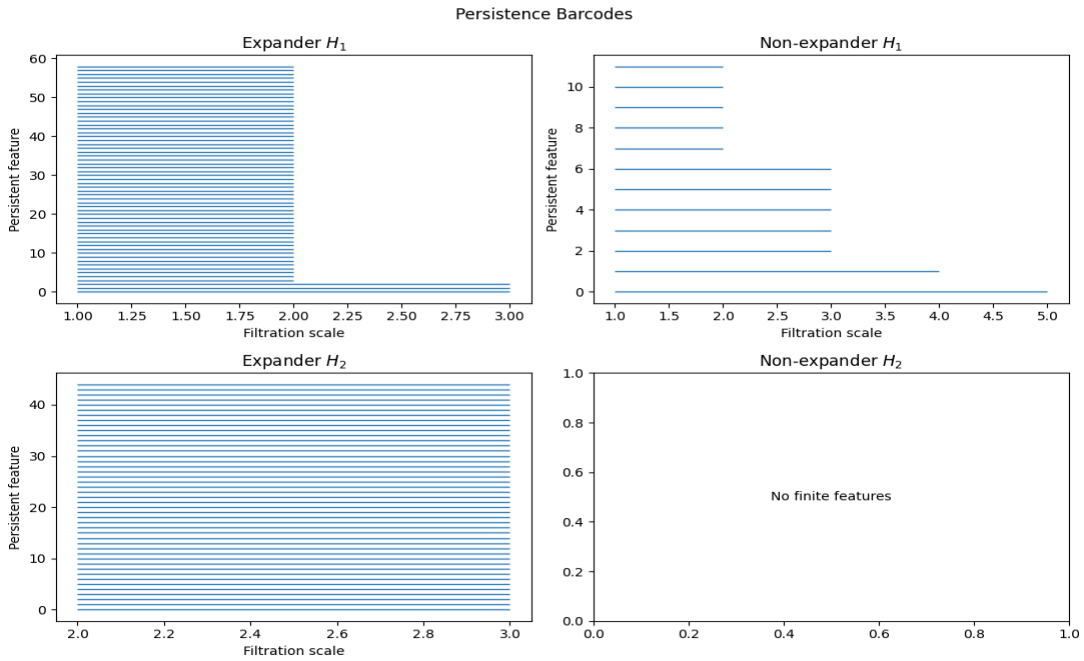

Figure 6. H_1 and H_2 persistence barcodes for representative controlled graphs.

The representative expander has a total of 59 features in H_1, having a persistence value of 62 and a total of 45 features in H_2 visible in the displayed figure. The representative non-expander, on the other hand, has 12 features in H_1 and 0 finite features in H_2.

The development of Betti numbers as the normalized filtration scales is illustrated in Figure 7.

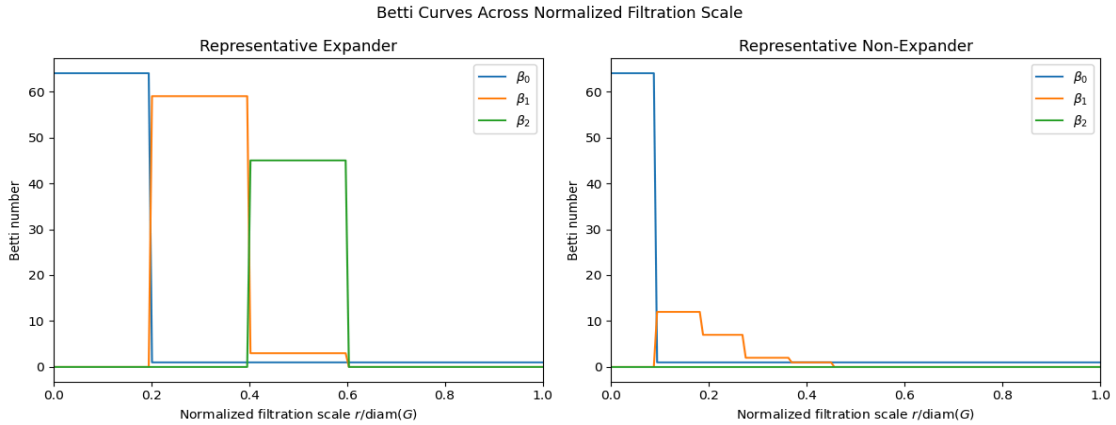

Figure 7. Betti curves across normalized filtration scale.

The Betti curves reveal an early rise in β_1 for both sample graphs. Moreover, the expander graph exhibits a strong β_2 phase over a medium normalized range of the filtration. This analysis represents the topology of the sample graphs without suggesting that all expanders exhibit such a persistence structure.

6.3 Expansion–Persistence Relationship

In the entire set of graphs, the persistence of H_1 total ranged significantly according to both type and degree of graph expansion. Mean persistence of H_1 total for controlled expanders was found to be 71.275, about three times that for controlled non-expanders at 20.042. However, the validation sample of real-world networks yielded a mean H_1 total persistence value of just 1.557, even though their mean spectral gap was higher. Thus, there does not seem to be any universal relationship where increase in λ_2 results in persistent homology.

The relation between spectral expansion and total H_1 persistence is illustrated in Figure 8.

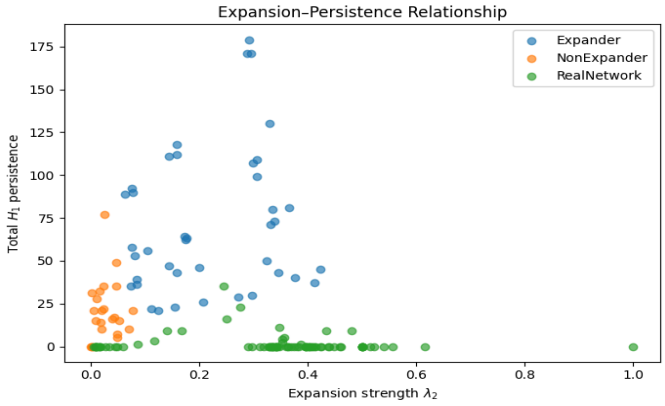

Figure 8. Expansion–persistence relationship across controlled and validation graph classes.

Figure 8 illustrates a wide area of high persistence in the H_1 persistence of the controlled expanders; however, real-world network data is close to zero. This indicates the significance of structural class in the interpretation of the relationship between spectral gap and persistent topology.

Figure 9 explores the possibility of the graph order as a factor.

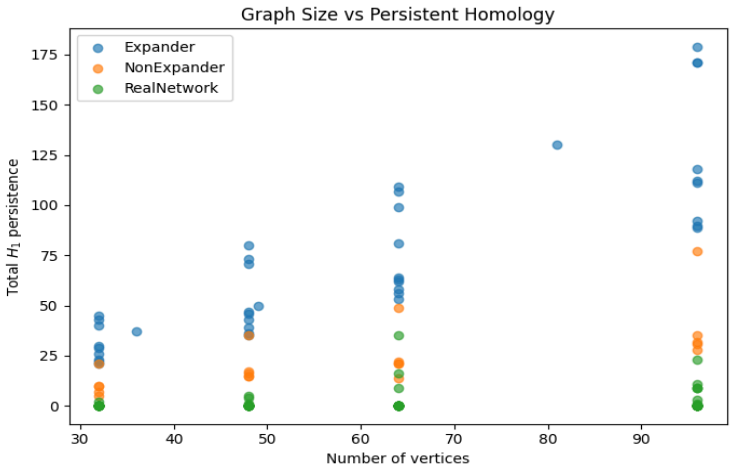

Figure 9. Graph size versus H_1 total persistence.

Figure 9 shows that there is a size effect present within the controlled set of graphs, such that larger graphs are able to accommodate more H_1 persistence overall, especially in expanders. The expansion-persistence relationship is thus to be viewed in conjunction with graph order and degree.

6.4 Homological Collapse

Definition of homological collapse was made operational through the identification of the last finite H_1 death scale. The mean H_1 collapse for expanders was 2.675 while the same for non-expanders was 5.958. The real-world network validation value was 0.318 since many networks had little to no H_1 structure remaining in them.

The connection between spectral expansion and collapse scales is depicted in figure 10 below.

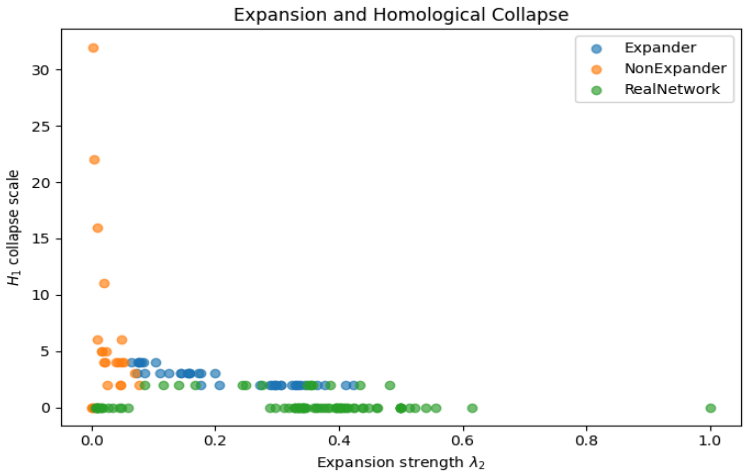

Figure 10. Expansion strength and H_1 homological collapse scale.

From Figure 10, it is clear that extremely large raw collapses scale is found in non-expanders where the expansion is weak, but the controlled expanders show a smaller low-collapse scale. Cycles are many at early scales in controlled expanders but are filled up in fewer graph distance.

For inferential analysis, there was use of Spearman rank correlation to measure monotonic correlation between spectral expansion and persistence results; Mann-Whitney U test to compare controlled expanders and non-expander results and HC3 robust ordinary least square regression to measure spectral gap correlation controlling for graph order and mean degree. The entire results are summarized in Table 3 below.

Table 3. Statistical analysis of expansion and persistent topology

Outcome	**Analysis**	**N**	**Estimate ($\rho/\beta/U$)**	**SE**	**p-value**	**Interpretation**
H_1 total persistence	Spearman correlation	152	$\rho = -0.3044$	—	<0.001	Significant negative monotonic association with spectral gap
H_1 total persistence	HC3 robust OLS: spectral gap	152	$\beta = -43.2738$	10.9584	<0.001	Significant negative association after adjustment for graph order and mean degree
H_1 total persistence	Mann–Whitney U	64 (40/24)	$U = 887.0$	—	<0.001	Controlled expanders have substantially higher H_1 total persistence than non-expanders
H_1 maximum lifetime	Spearman correlation	152	$\rho = -0.4481$	—	<0.001	Significant negative monotonic association with spectral gap
H_1 maximum lifetime	HC3 robust OLS: spectral gap	152	$\beta = -6.8179$	1.7887	<0.001	Higher spectral gap is associated with shorter maximum H_1 lifetime after adjustment
H_1 maximum lifetime	Mann–Whitney U	64 (40/24)	$U = 314.5$	—	0.0176	Controlled expanders have lower maximum H_1 lifetimes than non-expanders

H_1collapse scale	Spearman correlation	152	$\rho = -0.4481$	—	<0.001	Significant negative association between expansion and H_1 collapse scale
H_1collapse scale	HC3 robust OLS: spectral gap	152	$\beta = -8.3100$	1.9550	<0.001	Higher spectral gap is associated with earlier H_1collapse after adjustment
H_1collapse scale	Mann–Whitney U	64 (40/24)	$U = 314.5$	—	0.0176	Controlled expanders exhibit significantly earlier H_1collapse
Persistent-dimension index	Spearman correlation	152	$\rho = -0.3368$	—	<0.001	Significant negative pooled association with spectral gap
Persistent-dimension index	HC3 robust OLS: spectral gap	152	$\beta = -1.7291$	0.2754	<0.001	Spectral gap remains negatively associated with the operational dimension index after adjustment
Persistent-dimension index	Mann–Whitney U	64 (40/24)	$U = 658.0$	—	0.0085	Persistent-dimension index differs significantly between controlled graph classes
Effective feature number	Spearman correlation	152	$\rho = -0.2738$	—	<0.001	Significant negative pooled association between spectral gap and effective feature number
Effective feature number	HC3 robust OLS: spectral gap	152	$\beta = -36.3363$	10.0435	<0.001	Higher spectral gap is negatively associated with effective feature number after adjustment
Effective feature number	Mann–Whitney U	64 (40/24)	$U = 913.0$	—	<0.001	Controlled expanders have substantially larger effective feature numbers than non-expanders

Note: The Spearman correlation and HC3 regressions consider the full ensemble (N=152) with controlled expanders, controlled non-expanders, and network-validation examples. The robust HC3 OLS regressions take spectral gap, order of the graph, and average degree as predictors, where the reported values for βand SE pertain only to the spectral gap predictor. The Mann–Whitney U tests are limited to 40 expanders and 24 non-expanders (N=64).

Negative correlations were found between spectral gap and H_1 total persistence, H_1 maximum lifetime, H_1 collapse scale, persistent-dimension index, and effective number of features in all 152 cases. Negative correlations of the spectral gap remained true for the spectral gap coefficient in the HC3 models even after adjusting for graph order and average degree. However, for the class-controlled comparison, there were significantly larger values of H_1total persistence and effective number of features in the case of expanders, together with significantly shorter H_1maximum lifetimes and earlier collapse times. This discrepancy between the two results is due to the heterogenous real-network validation part.

6.5 Stability Results

The stability test included 240 perturbation tests. The mean bottleneck distance and mean Wasserstein distance grew steadily with an increase in the amount of perturbation. The bottleneck distance ranged from about 0.015 for the smallest perturbation to 0.147 for ε = 0.10, while the Wasserstein distance ranged from about 0.34 to 3.44.

Figure 11 demonstrates the stability test results.

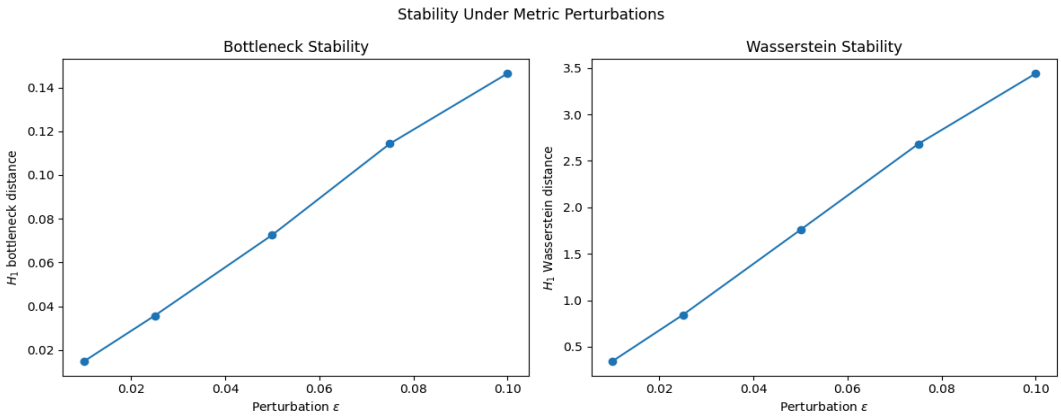

Figure 11. Stability of H_1 persistence under controlled metric perturbations.

The graphs show that there is an increase in the distance between the persistence diagrams when the perturbation size increases. The response is monotonous in nature, implying that there is a controlled variation in persistence as opposed to instability.

6.6 Dimensional Reduction

The difference between the classes is significant regarding persistence entropy and effective topological complexity. The controlled expanders have the average H_1 entropy of 3.9145, while for the average entropy-effective feature number it is equal to 71.9945. The non-expanders have the average H_1 entropy of 1.6533 and entropy-effective feature number of 13.6578. As for real networks, the mean H_1 entropy is equal to 0.2891, while the mean entropy-effective feature number is 1.6023.

Differences in classes concerning persistence entropy and effective complexity are demonstrated in Fig. 12.

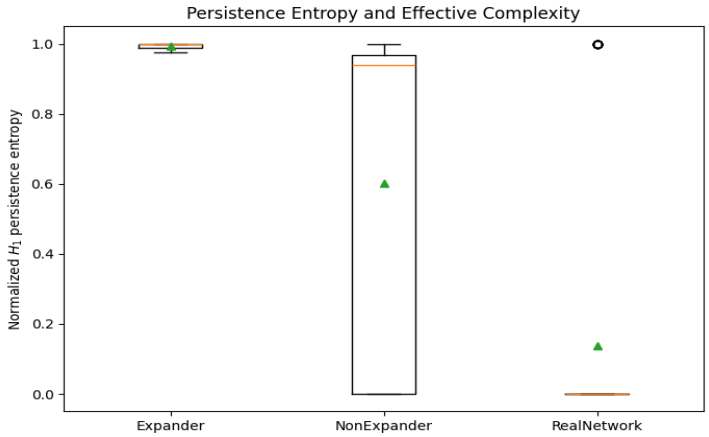

Figure 12. Persistence entropy and effective complexity across graph classes.

Figure 12 shows significantly higher persistence entropy and effective complexity of features for the controlled expanders compared to the external real networks, while the controlled non-expanders lie somewhere in between.

The dependence of the spectral expansion on the operational dimension is illustrated by Figure 13.

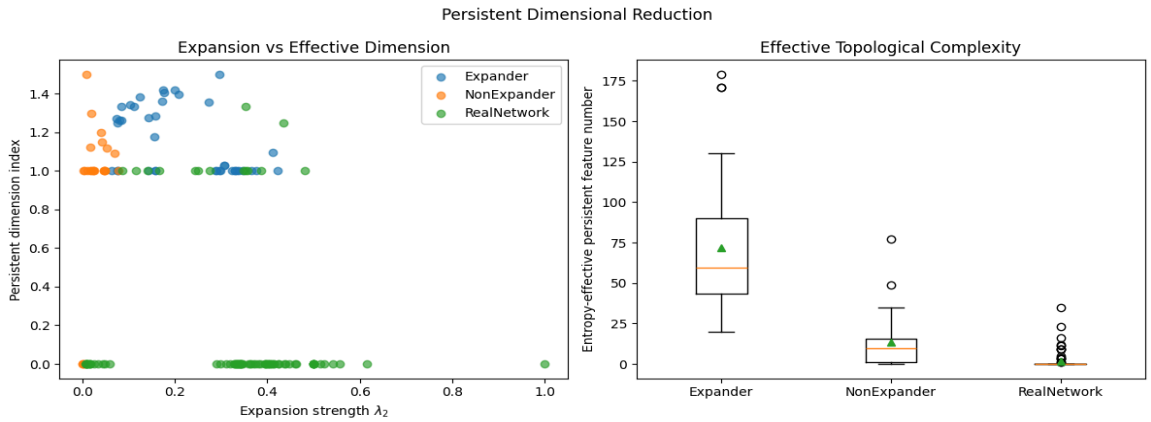

Figure 13. Persistent dimensional reduction: expansion versus operational dimension and effective topological complexity.

As Figure 13 shows, expansion, operational persistent dimension, and topological complexity differ from each other among graph classes. The synthetic expanders show much higher levels of effective persistent complexity in comparison with the real network examples even in view of the higher spectral gap in the latter.

Table 4 shows the results for dimensions and entropy.

Table 4. Dimensional and entropy summaries

Class	**Mean H_1 entropy**	**Mean H_2 features**	**Mean persistent-dimension index**	**Mean effective features**
Expander	3.9145	10.1500	1.1546	71.9945
Non-expander	1.6533	1.5000	0.8951	13.6578
Real network	0.2891	0.0455	0.1657	1.6023

Note: H_2 summaries are based only on graph instances for which H_2 computation was feasible; consequently, H_2-based quantities should not be interpreted as uniformly observed across the complete 152-instance ensemble.

For the operational persistent dimension index, the values were highest for the controlled expanders (1.1546) on average, followed by the controlled non-expanders (0.8951), then the real network samples (0.1657). This measure reflects the lifetime mass concentration over the homological dimensions calculated and should not be mistaken as the intrinsic dimension invariant. From the PCA analysis, PC1 accounts for 38.6% of the standard structural-persistent variance while PC2 accounts for 31.4% to give 70% together.

6.7 Supplementary Structural and Stability Diagnostics

Additional tests were performed to determine the relationships between graph size, metric compactness, persistence indicators, perturbation robustness, and low-dimensional structure-persistence organization. The additional tests provide more insight into how the identified persistence properties are related to other structural properties.

Graph diameter as a function of graph order is shown in Figure 14.

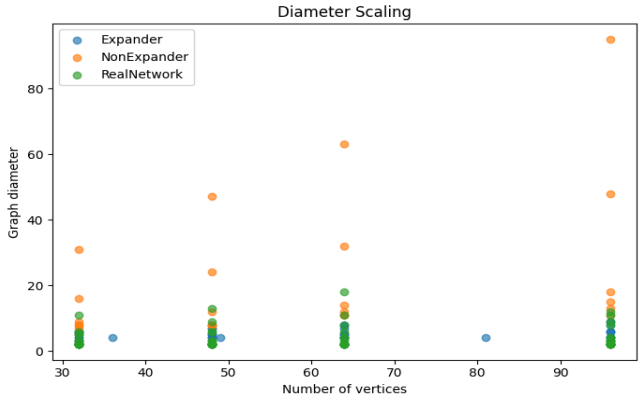

Figure 14. Diameter scaling with graph order.

Figure 14 distinguishes between the elongated non-expanders and the small controlled expanders, as well as most real-world network examples. This outcome is in agreement with the significant difference in average diameter for each class shown in Table 2.

The full set of rankings with respect to structural and persistent properties is provided in Figure 15.

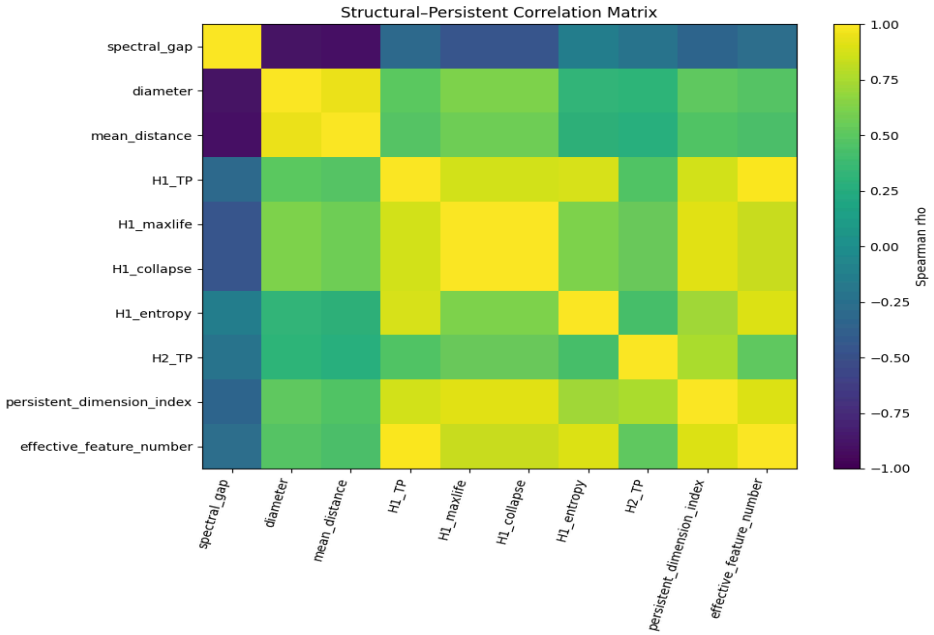

Figure 15. Spearman structural–persistent correlation matrix.

As illustrated in Figure 15, there is high correlation between diameter, average distance, lifetime of H_1, entropy, H_2, and operational dimension. There is negative correlation between spectral gap and several raw distances/persistence values for the pooled ensemble. Since each graph class plays distinct experimental roles, the correlations found in the pooled ensembles are treated as descriptive.

The correlation between persistence displacement and metric distortion is presented in Figure 16.

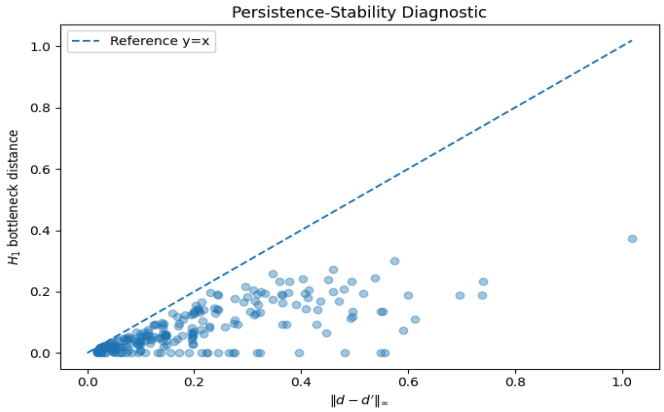

Figure 16. Persistence-stability diagnostic: H_1 bottleneck distance versus metric distortion.

The observed bottleneck distances are still under the y=x reference line in the shown range. Hence, in all the perturbation experiments conducted, persistence offset was still less than the maximum metric distortion that was measured, hence giving another way of testing for stability besides the graphs in figure 11.

Lastly, the structural-persistent dataset is depicted in a reduced form in figure 17.

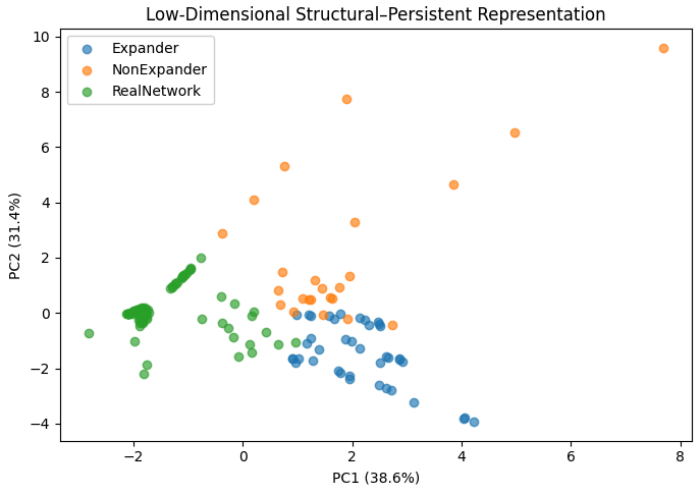

Figure 17. Low-dimensional structural–persistent PCA representation.

Class separation is observable to an extent in the PCA visualization. The controlled expanders appear in a relatively tight cluster, while the non-expanders are spread out along both axes. The PCA representation, together with the 70.0% variance captured in the two primary components, is thus a succinct, low-dimensional description of the properties of the ensemble graph.

7. DISCUSSION

The results indicate that metric expansion and persistent topology have a relationship with each other, through an interplay of spectral connectivity, shortest-path geometry, feature richness, persistence duration and collapse dynamics. Controlled expanders had significantly more H_1-features than non-expanders, while the individual features in them tended to disappear much faster at lower filtration values. The validation on real networks also demonstrated that spectral gap in itself was not a sufficient measure of persistent complexity.

7.1 Main Findings

Controlled expanders showed an average H_1 total persistence of 71.2750, while the corresponding value for non-expanders was 20.0417. In addition, controlled expanders showed an increased number of H_1 features on average (63.0000 vs. 13.1667). Their average maximum lifetime of H_1 was smaller (1.6750 vs. 5.1250) and they collapsed at a smaller average scale (2.6750 vs. 5.9583). It appears that expanders have many H_1features of short duration.

Real-network examples behave differently. Even though they had the highest spectral gap of all groups (0.3206), their average H_1total persistence was the lowest (1.5568). It means that spectral expansion alone does not determine persistence; heterogeneity of degree distribution, clustering, hubs, and sampling scheme.

7.2 Expansion and Topology

The controlled findings highlight the key difference between feature abundance and feature longevity. Sparse expanding graphs are able to produce many H_1cycles at small filtration scales, creating high total persistence. At the same time, due to their high global connectivity, expanding graphs have short metric paths, which enable higher dimensional simplices to close the cycles fast. Non-expanders showed the contrary tendency: lower persistence but higher individual lifespans due to the longer graph distances that hindered simplicial filling.

Such a difference is also present in the statistical sense. The controlled expanders demonstrated significantly higher total persistence of H_1cycles compared to non-expanders ($U=887.0$, $p<0.001$). In the analysis of the pooled sample consisting of 152 instances, however, the spectral gap correlated negatively with the total persistence of H_1cycles ($\rho=-0.3044$, $p<0.001$).

7.3 Stability and Collapse

Controlled expanders experienced earlier H_1 collapse compared to non-expanders, with mean collapse scales of 2.675 and 5.958. A statistically significant difference was observed ($U=314.5$, $p=0.0176$). Do not interpret early collapse as a lack of topology. Expanders contain many features at first, but they have a compact metric geometry such that those features are filled within relatively few filtration steps.

The 240 metric perturbation runs exhibited stable behaviour. As Epsilon increases from $\varepsilon=0.10$ to 0.10 mean bottleneck distance increases from 0.015 to 0.147 while mean Wasserstein distance increase from 0.34 to 3.44. The gradual response indicates that the persistence diagrams changed not abruptly, but rather that the system gradually became unstable.

7.4 Dimensional Reduction

Different classes of graphs differed sharply from each other in terms of persistent complexity. Controlled expanders had a mean H_1 entropy of 3.9145, mean persistent-dimension index of 1.1546, and mean effective feature number of 71.9945. For non-expanders, the values were 1.6533, 0.8951, and 13.6578 and for real networks, they were 0.2891, 0.1657 and 1.6023. In instances where H_2computation was viable, controlled expanders also exhibited, on average, greater H_2features.

The PCA results revealed that PC1 and PC2 described the standardized structural–persistent variance by 38.6% and 31.4%, respectively, taken together 70.0%. These findings suggest that dimensional reduction acts as an operational representation of persistent complexity, not an intrinsic-dimension theorem.

7.5 Comparison with Previous Studies

These scale-dependent phenomena are in agreement with research which showed that Vietoris–Rips topology is highly dependent on the metric geometry and filtration scale of the space. Scale-dependent topological and connectivity transitions in Vietoris–Rips complexes were shown by Moy (2023) and Adams et al. (2025). In the current paper, these scale-dependent phenomena have been extended to the case of expander metrics generated by a graph structure, where many initial persistent homology features exist alongside fast collapse of the simplicial complex.

The smooth response to perturbation is also in line with stability considerations from the theory of persistent summaries stated by Atienza et al. (2020). Geometric expansion, on the other hand, has also been studied in a more general context than just graphs (Winkel, 2021), while TDA computational platforms facilitate the use of persistent summaries together with low-dimensional data (Tauzin et al., 2021).

7.6 Theoretical Contributions

The Study offers a comprehensive analysis of the four concepts, namely, spectral expansion, metric geometry, persistent homology and effective topological complexity. The important concept presented in the paper is the separation of topological abundance from topological survival. In this respect, controlled expanders exhibited feature abundance and persistence in the total but shorter individual lifespan and premature decay as compared to non-expanders.

Additionally, the external validation shows that spectral gap cannot be considered an independent predictor of persistent complexity since one should consider the family of graphs, connectivity, degree and shortest-path geometry as well.

7.7 Study Limitations

The research is constrained to the cases of finite graph size with controlled graph order varying between 32 and 96 nodes. Computation of H_2 persistent homology was only possible for a particular sub-sample of the smaller graphs and hence

limiting the ability of a comparative analysis of all samples. The results are subject to the chosen expander/non-expander graph sets as well as the selected connected subsets of the external graphs.

Further, persistent dimension and persistent dimension index are effective measures and not intrinsic-dimension invariants. Therefore, their properties need to be studied for different sets of graphs and parameters.

8. CONCLUSION AND RECOMMENDATIONS

The current study developed a framework for investigating the relationships between spectral expansion, graph-induced metric geometry, and persistent topology, including analyses on 152 graph cases: 40 controlled expanders, 24 controlled non-expanders, and 88 real-network validations. It was found that controlled expanders had significantly more total H_1persistence than non-expanders: 71.2750 and 20.0417, respectively; however, the mean H_1collapse scale was smaller for expanders than for non-expanders: 2.6750 and 5.9583. This suggests a fundamental difference between topological abundance and longevity: expanders have potential to create many topological features but because of its compact geometric structure, it can collapse earlier than non-expanders.

Furthermore, controlled stability analysis shows that bottleneck distance increases from 0.015 to 0.147, and Wasserstein distance from 0.34 to 3.44, as εincreases from 0.01 to 0.10. Real network validation results also revealed the point that spectral expansion itself is not a criterion for persistent topology, since relatively large spectral gap does not guarantee high H_1persistence. In summary, there are connections among expansion, persistence, collapse, stability, and effective dimensionality found in this computational study. Future extensions may include: large graph orders, additional construction of expanders, use of weighted metrics, and more persistent homology computation in higher dimensions.

9. FUTURE WORK

It is important that future studies apply this approach on large graph sequences and analyze H_2, H_3, and higher order homologies with computational techniques that can make Vietoris–Rips constructions less complex. Finite size effect found for graphs with number of vertices equal to 32 to 96 can also be analyzed from the asymptotic point of view in order to learn about evolution of persistence, collapse scales, and dimensionality for growing graph size. Additional studies of weighted and random expanders will clarify the influence of combinatorics as compared to metrics. Finally, the persistent dimension measures used in this study have to be developed theoretically and analyzed along with other scaling laws and persistent features.

REFERENCES

1. Adamaszek, M., & Adams, H. (2022). On Vietoris–Rips complexes of hypercube graphs. *Journal of Applied and Computational Topology*, *6*(2), 177-192. https://doi.org/10.1007/s41468-021-00083-1

2. Adamaszek, M., Adams, H., Gasparovic, E., Gommel, M., Purvine, E., Sazdanovic, R., ... & Ziegelmeier, L. (2020). On homotopy types of Vietoris–Rips complexes of metric gluings. *Journal of Applied and Computational Topology*, *4*(3), 425-454. https://doi.org/10.1007/s41468-020-00054-y

3. Adams, H., Bush, J., & Virk, Ž. (2025). The connectivity of Vietoris–Rips complexes of spheres: H. Adams et al. *Journal of Applied and Computational Topology*, *9*(2), 15. https://doi.org/10.1007/s41468-025-00214-y

4. Arya, S., Boissonnat, J. D., Dutta, K., & Lotz, M. (2021). Dimensionality reduction for k-distance applied to persistent homology. *Journal of Applied and Computational Topology*, *5*(4), 671-691. https://doi.org/10.1007/s41468-021-00079-x

5. Atienza, N., González-Díaz, R., & Soriano-Trigueros, M. (2020). On the stability of persistent entropy and new summary functions for topological data analysis. *Pattern Recognition*, *107*, 107509. https://doi.org/10.1016/j.patcog.2020.107509

6. Bauer, U. (2021). Ripser: efficient computation of Vietoris–Rips persistence barcodes. *Journal of Applied and Computational Topology*, *5*(3), 391-423. https://doi.org/10.1007/s41468-021-00071-5

7. Brito, G., Dumitriu, I., & Harris, K. D. (2022). Spectral gap in random bipartite biregular graphs and applications. *Combinatorics, Probability and Computing*, *31*(2), 229-267. https://doi.org/10.1017/S0963548321000249

8. Chachólski, W., Jin, A., Scolamiero, M., & Tombari, F. (2021). Homotopical decompositions of simplicial and Vietoris Rips complexes. *Journal of Applied and Computational Topology*, *5*(2), 215-248. https://doi.org/10.1007/s41468-021-00066-2

9. Dinitz, M., Schapira, M., & Shahaf, G. (2020). Approximate Moore graphs are good expanders. *Journal of Combinatorial Theory, Series B*, *141*, 240-263. https://doi.org/10.1016/j.jctb.2019.08.003

10. Lim, S., Memoli, F., & Okutan, O. B. (2024). Vietoris–Rips persistent homology, injective metric spaces, and the filling radius. *Algebraic & Geometric Topology*, *24*(2), 1019-1100. https://doi.org/10.2140/agt.2024.24.1019

11. Majhi, S. (2023). Vietoris–Rips complexes of metric spaces near a metric graph. *Journal of Applied and Computational Topology*, *7*(4), 741-770. https://doi.org/10.1007/s41468-023-00122-z

12. Moy, M. (2023). Vietoris–Rips metric thickenings of the circle. *Journal of Applied and Computational Topology*, *7*(4), 831-877. https://doi.org/10.1007/s41468-023-00130-z

13. Oudot, S., & Solomon, E. (2021). Barcode embeddings for metric graphs. *Algebraic & Geometric Topology*, *21*(3), 1209-1266. https://doi.org/10.2140/agt.2021.21.1209

14. Sarid, A. (2023). The spectral gap of random regular graphs. *Random Structures & Algorithms*, *63*(2), 557-587. https://doi.org/10.1002/rsa.21150

15. Shukla, S. (2023). On Vietoris–Rips complexes (with scale 3) of hypercube graphs. *SIAM Journal on Discrete Mathematics*, *37*(3), 1472-1495. https://doi.org/10.1137/22M1481440

16. Skraba, P., & Turner, K. (2020). Wasserstein stability for persistence diagrams. *arXiv preprint arXiv:2006.16824*. https://doi.org/10.48550/arXiv.2006.16824

17. Tauzin, G., Lupo, U., Tunstall, L., Pérez, J. B., Caorsi, M., Medina-Mardones, A. M., ... & Hess, K. (2021). giotto-tda:: A topological data analysis toolkit for machine learning and data exploration. *Journal of Machine Learning Research*, *22*(39), 1-6. https://jmlr.org/papers/volume22/20-325/20-325.pdf

18. Vipond, O. (2020). Multiparameter persistence landscapes. *Journal of Machine Learning Research*, *21*(61), 1-38. https://jmlr.org/papers/volume21/19-054/19-054.pdf

19. Wagner, U. (2022). High-dimensional expanders (after Gromov, Kaufman, Kazhdan, Lubotzky, and others). *Bulletin de la Societe Mathematique de France*, *438*. https://doi.org/10.24033/ast.1188

20. Winkel, J. (2021). Geometric property (T) for non-discrete spaces. *Journal of Functional Analysis*, *281*(8), 109148. https://doi.org/10.1016/j.jfa.2021.109148